
Article:
Yi, C.Y. and Peng, C. orcid.org/0000-0001-8199-0955 (2017) Correlating cooling energy use with urban microclimate data for projecting future peak cooling energy demands: Residential neighbourhoods in Seoul. Sustainable Cities and Society, 35. pp. 645-659. ISSN 2210-6707

https://doi.org/10.1016/j.scs.2017.09.016

Correlating cooling energy use with urban microclimate data for projecting future peak cooling energy demands: Residential neighbourhoods in Seoul

Choo Yoon Yi and Chengzhi Peng*

School of Architecture, University of Sheffield, Arts Tower, Western Bank, Sheffield S10 2TN, UK

cyyi1@sheffield.ac.uk; c.peng@sheffield.ac.uk

*Corresponding author

[Manuscript accepted for publication by Sustainable Cities and Society, 17/09/2017]

Abstract

The paper presents a relational study of correlating cooling energy use with local weather station and apartment price data in Seoul. The overall analysis at a macro-level shows monthly variations in the correlation coefficients of cooling energy use and local weather station data during summer months. A further analysis at a micro-level shows temporal and spatial variations in the correlation. As the August correlation appears the strongest across all city districts, up to r=.972, a simple bivariate regression (SBR) model is derived to predict peak cooling energy use for each district. Given the latest climate change projections for Seoul, we use the SBR models to estimate increases of cooling energy use for each city district in August 2050s. The largest predicted increase rate (IR) is 96.1% in one city district (from 124.5% in 2012 to 220.6% in 2047). The smallest IR is 6.0% in another city district (from 51.5% to 57.5%). In 2047, the city district with the highest predicted IR is up to 292.8%, while the lowest is up to 57.5%. We discuss the implications of the projected future peak cooling energy demands for sustainable resilience as well as citizen's health and wellbeing.

Keywords

Residential cooling energy use; urban microclimate; property price; relational study; linear regression model; climate change projections

1. Introduction

Better understanding energy use in residential buildings for cooling is becoming increasingly important from the perspective of climate change even in heating-dominant countries. Intuitively, residential cooling energy use is largely related to weather conditions as buildings interact with their immediate surroundings. However, looking beneath the overall city level, the scene is much more complex. Not all cooling energy use can be neatly characterised into some uniformity. How does cooling energy use in urban residential buildings correlate

with urban weather? Can any such correlation be reliably drawn through collecting and examining field measurements? To what extent, is the correlation spatial-temporal specific? A better understating of these questions will improve our ability to project cooling energy demands in future climate scenarios to inform longer-term energy policy making. Furthermore, a robust projection capability is more likely to be applied to planning and design of urban neighbourhoods and buildings, either retrofitting or constructing new ones.

We have identified that Seoul is the only city in the world where the datasets from field measurements required to address our research questions have been made publicly available. Our research aims to develop a methodological framework for analysing open heterogeneous datasets and deriving correlational models that could project future cooling energy demands of urban residential neighbourhoods at a micro-climatic scale (up to 1 km). Using Seoul's city districts as case studies, we expect that the proposed methodological framework can be applicable to other cities for site-specific analyse and modelling as long as these cities start similar data collections and make them accessible to researchers.

2. Theory and Open Data

2.1. Factors affecting cooling energy use in residential buildings

Yu and co-workers (2011) identified several factors as major determinants affecting energy use in residential buildings which can be categorised into three groups: (a) climate, e.g. external temperatures; (b) building physical environment, e.g. building envelop and service systems; and (c) user related aspects such as occupants' behaviours, activities and socio-economic statuses. As informed by more recent studies, we consider climate change an important additional factor that takes into account the likely effects of rising outdoor ambient temperature and increased frequencies of heatwave on cooling energy demand.

Firstly, climate is one of the most significant factors affecting building thermal and energy performance. Of the wide range of climate variables, air temperature, humidity, wind pattern (speed and direction) and solar radiation are considered the most significant parameters (Flor & Domınguez, 2004). Especially, dry-bulb temperature is one of the most influential climatic variables in measuring heating and cooling degree days (HDDs and CDDs) (Lee & Levermore, 2010), which affects building energy use. Flor and Dominguez (2004) investigated the impacts of microclimate on building energy use through modification of weather variables based on an integrated computational model. Allegrini et al. (2012) studied influence of microclimate, effect of neighbouring buildings in street canyon, on building heating and cooling demand using building energy

simulation. Moonen et al. (2012) reviewed and highlighted the importance of investigation of urban microclimate to assess building energy demand, and several other authors suggested outdoor and indoor integrated or coupling assessment methods based on computational model as a solution to improve building energy use and the accuracy of the assessment (He et al., 2009; Bouyer et al., 2011; Yang et al., 2012). Despite of the importance of microclimate for assessing building energy use, very few studies have been carried out to investigate interrelations between microclimate and building energy use (Asimakopoulos et al., 2001), especially involving actual field measurements in residential buildings. Santamouris et al. (2001) investigated urban climate impacts on building energy use based on climatic measurements from almost 30 urban and suburban stations, which was conducted with one representative office building for all locations. Other related studies for residential buildings have been carried out, using alternative inputs rather than location-specific weather data, e.g. city-wide HDDs and CDDs for the energy modelling study (Aydinalp et al., 2002) and weather normalization process based on equation of line-of-best fit between HDDs (and CDDs) and energy use dataset for energy correlation study (Touchie et al., 2013).

The importance of microclimatic consideration on building energy use is owing to diversity of urban weather conditions such as Urban Heat Island (UHI). UHI is often considered as the most typical example of anthropogenic climate modifications, resulting from the energy (heat) interactions between urban surfaces and the ambient atmospheric layers (Arnfield, 2003; Rizwan et al., 2008). For the period 1999-2002 in Seoul, Lee and Baik (2010) found that the maximum daily UHII during non-precipitation days (and precipitation days) was observed to 4.5^{o}C (2.6^{o}C) in spring, 3.5^{o}C (2.4^{o}C) in summer, 4.8^{o}C (3.2^{o}C) in autumn and 4.5^{o}C (3.2^{o}C) in winter. At the building level, the effect of UHI creates site-specific microclimate conditions and they in turn have significant impacts on building energy use, especially on summer cooling. Santamouris et al. (2001) and Kolokotroni et al. (2006) studied the effect of urban heat island on cooling energy use in office buildings in Athens and London respectively: in Athens, where the mean UHII exceeded 10^{o}C, the urban cooling load was double of rural buildings; in London, the cooling energy demand of rural reference building was 84% of urban and there was no cooling demand investigated in the optimised rural building, maintaining indoor temperature below 24^{o}C. To improve building energy assessment, Chan (2011a) highlighted using the site-specific modified typical meteorological year (TMY) weather file as a weather input in building simulation to reflect diversity of urban weather, such as the UHI; applying the modified weather input in the Hong Kong case study, there was about 10% increase in air-conditioning demand compared to the existing TMY in both office building and residential flat. More closely related to our current study, Salvati et al. (2017) reported the UHI impacts on

residential cooling energy use in Barcelona: the maximum UHI intensity at street level was 4.3°C, and its impact on sensible cooling load was estimated to increase of 18%-28%.

Secondly, energy use in the residential building sector is also affected by user-related factors, such as residents' behaviour (Yun and Steemers, 2011), occupant age (Chen et al., 2013) and socio-economic circumstances (Schuler et al., 2000). However, the strength of these factors varies by location and the type of energy use (e.g. heating or cooling). Resident behaviour was influential for cooling in the US (Yun and Steemers, 2011), and occupant age was found more significant than income for both heating and cooling in Hangzhou, China (Chen et al., 2013). Socio-economic characteristics were found significant but less influential than building physical characteristics for heating in western Germany (Schuler et al., 2000). In the Netherlands, occupant characteristics and behaviour explained only 4.2% variation for heating while building characteristics explained 42% (Santin et al., 2009). As the literature reviewed have shown that user related aspects could play a role but such influence might be inconclusive depending on location and energy use type, our study therefore included the property price data of apartment buildings in Seoul as a socio-economic indicator reflecting to some extent the residents' cooling energy use decisions.

Thirdly, the impact of climate change on building energy use has been investigated by many researchers world-wide, some of which focussed on residential buildings. Wilde and Coley (2012) reviewed the known impacts on residential buildings in the UK (Gaterell & McEvoy, 2005; Hacker et al., 2008; Collins et al., 2010), in Switzerland (Frank, 2005), in Australia (Wang et al., 2010), and in Hong Kong (Chan, 2011b). Li et al. (2012) reviewed the impacts in different climate zones and highlighted the most significant impacts would be seen where hot summer and warm winter climates occur. Quantitatively, Crawley (2008) estimated that the overall energy use would increase by more than 20% from the current level in 'tropical' climates; and in middle latitude climates, it would reduce by 25% for heating and increase by 15% for cooling. In South Korea, Chung et al. (2004) found that the increase of annual mean temperature during 1974-2002 was 1.5°C in Seoul, while the increase in the rural area was 0.6°C. Also, there was 259 mm increase of precipitation during the last century. Wang et al. (2007) analysed 227 years daily precipitation records in Seoul and found that there was increase of mean summer precipitation between the Cheugugi period (1778-1907) and the modern period (since 1908): the former was 861.8 mm whereas the latter was 946.5 mm. Moreover, during the past 20 years, the torrential rain frequency data showed that the torrential rain was increased to 25% and heavy rain warning was increased to 60% (Seo & Lee, 2011). According to the Fifth-Generation Penn State/NCAR Mesoscale Model (MM5, Grell

et al., 1994) climate change projection downscaling for South Korea, the temperature during the summer period of 2071-2100 was predicted to increase 5.5°C with reference to 1991-2000 (Boo et al., 2006).

2.2. Seoul's open data

The City of Seoul consists in 25 "*gu*" (districts), and each city district contains a number of "*dong*" (administrative neighbourhoods). We first analyse Seoul's open data to search for potential correlations between (a) the actual residential cooling energy use extracted from the energy bill data from the apartment neighbourhoods, and (b) the actual location-specific microclimate urban weather data as measured from the city district (CD) automatic weather stations (AWS).

2.2.1. Urban microclimate data

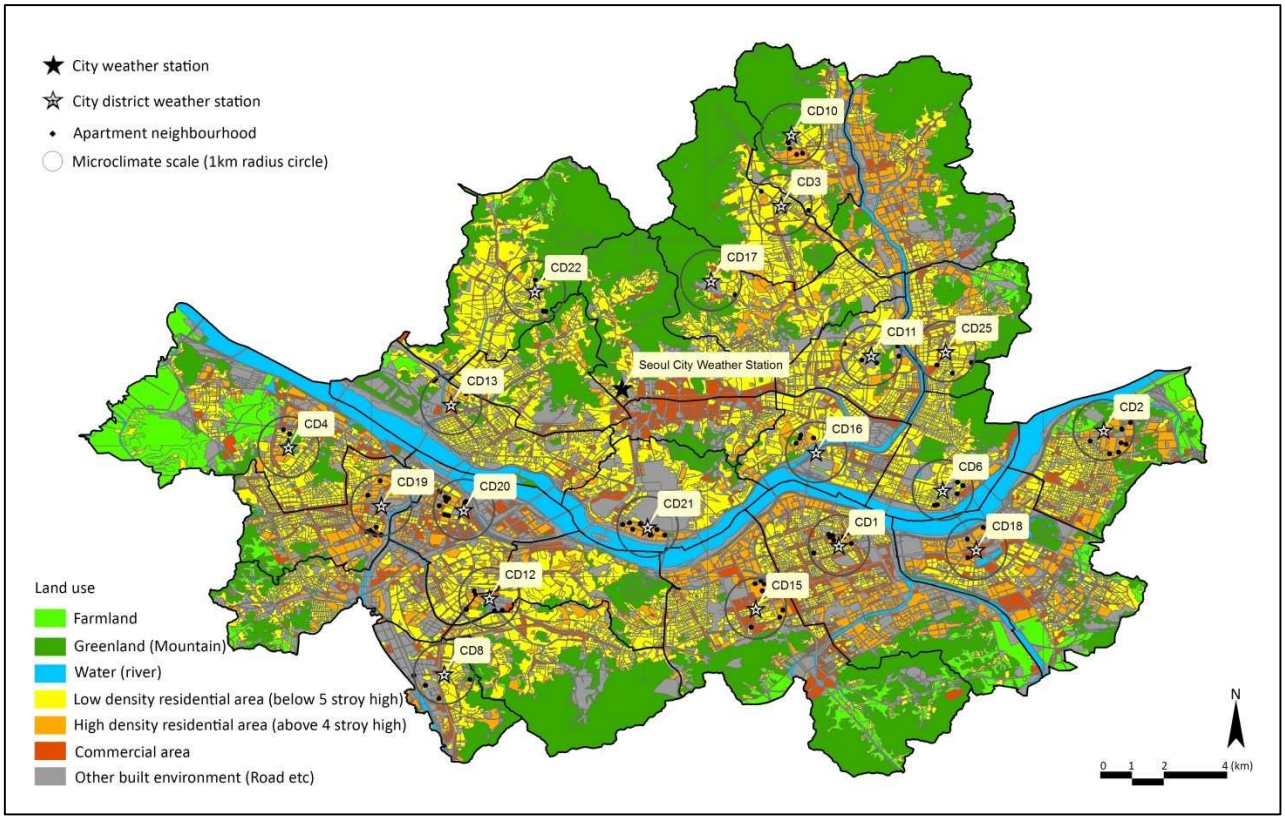

Figure 1. Locations of the 98 apartment neighbourhoods (AN) within 1km radius of the 19 city district (CD) automatic weather stations (AWS) in Seoul identified for the study.

The urban microclimate data collected at the AWS of each city district in Seoul are publicly available (KMA, 2017; MDOP, 2016). However, the scope of AWS data is limited to temperature (dry-bulb), wind direction/speed and precipitation (above 0.5mm). As dry-bulb temperature is the most influential weather

variable affecting building thermal conditions and energy use, it was chosen to represent the urban weather data in this study. Figure 1 shows the locations and boundaries of the 19 city districts identified, considering the sample size for statistical analyses (see 2.2.2). The boundary of 1km radius within the AWS location is set according to the spatial scale of urban microclimate (Oke, 2006). Thus, a total of 98 apartment neighbourhoods (*Danji*) are identified across the 19 district sites. Table 1 shows the locations of the 19 AWS, including height (above sea level), estimated street and building roof level and the associated neighbourhood information such as apartment building height and size. However, as the AWS data contain only location and height above sea level, the street level was estimated from the roof floor level with 3m for average floor height. As most of the CD AWS are installed on building roof tops, the collected temperature data could be regarded as an influential weather variable affecting cooling energy use of the associated neighbourhoods. It should be pointed out here that the CD AWS datasets encompass urban heat island (UHI) effects wherever and whenever present in the district areas.

Table 1. The location information of City District (CD) Automatic Weather Station (AWS), and height and size information of the Apartment Neighbourhood (AN) within each CD-AWS 1km boundary

	CD AWS info.					AN info.			
	Location		Height info.						
	Lat.	Long	Sea lv. (m)	Street lv. (m)	Roof lv. (Stories)	Avg. Top floor lv.	Avg. Min floor lv.	No. Apt. Building	No. Apt.
CD1	37.5134	127.0470	59.6	50.6	3	21	13	59	4193
CD2	37.5555	127.1450	56.9	47.9	3	17	12	61	4977
CD3	37.6397	127.0257	55.7	34.7	7	17	12	15	1517
CD4	37.5499	126.8425	79.1	64.1	5	20	13	64	3519
CD6	37.5336	127.0853	38.0	38.0	0	19	11	16	1692
CD8	37.4655	126.9001	41.5	29.5	4	21	15	30	2156
CD10	37.6661	127.0295	55.5	43.5	4	14	11	47	4862
CD11	37.5846	127.0604	49.4	34.4	5	21	11	47	3387
CD12	37.4937	126.9181	33.8	33.8	0	19	15	17	2049
CD13	37.5655	126.9027	25.0	13.0	4	16	10	18	1192
CD15	37.4889	127.0156	35.5	26.5	3	17	10	67	6565
CD16	37.5472	127.0388	33.7	18.7	5	17	10	25	2065
CD17	37.6117	126.9994	125.9	107.9	6	19	11	37	3033
CD18	37.5115	127.0967	53.6	29.6	8	18	15	105	11276
CD19	37.5296	126.8782	9.7	6.7	1	18	9	119	7892
CD20	37.5271	126.9070	24.4	12.4	4	21	15	52	3980
CD21	37.5204	126.9761	32.6	20.6	4	21	13	52	4681
CD22	37.6077	126.9338	65.0	56.0	3	16	8	34	1976
CD25	37.5855	127.0868	40.2	28.2	4	18	12	11	1087

2.2.2. Cooling energy use data

Similar to Hong Kong and other Asian mega cities, the typical type of residential buildings in Seoul is high-rise apartment buildings. According to the Korean Statistical Information Service (KOSIS, 2013), nearly 50% of residential buildings are of the apartment type nationally. In Seoul, 42.55% of residential buildings are apartments. Also, about 84% of apartments are tall buildings over 10-story high. The number of households in each apartment neighbourhood can be widely different from hundreds to thousands. Also, the floor area of an

apartment unit varies, typically from 59.4 m^2 to 148.4 m^2 according to KOSIS (2013), indicating diverse family sizes. Due to the very high ratio of apartment buildings in South Korea, the Ministry of Land, Infrastructure and Transport (MoLIT) established the Apartment Management Information System (AMIS, 2010).

The AMIS was designed to inform the monthly energy bill of each apartment neighbourhood including gas and electricity usage. For our study, in order to extract cooling energy use data from the AMIS, the electricity bill data was chosen among other types of energy bills as only the electricity bill reflects energy use for summer cooling in Seoul (i.e. uses of household air-conditioning and electric fans). Notably, the AMIS energy bill data is an average monthly energy bill of each apartment neighbourhood not a single residential household's monthly energy bill. Therefore, the collected electricity bill data from each apartment neighbourhood (Korean Won per square metre, KRW/m2) reflects collective energy use for summer cooling specific to the neighbourhood location.

According to the Korea Electric Power Corporation (KEPCO, 2016), the only electric power supplier in South Korea, currently 95% of total apartments in South Korea have the same metre reading day (18^{th} of each month). We therefore assume that 95% is sufficient for all apartments in our statistic relational study to have the same metre reading day. Considering their sample sizes, city districts containing less than 3 apartment neighbourhoods were not included in this study. Thus, 19 city districts and a total of 98 apartment neighbourhoods (approx. 72,000 apartment households) were identified for the study, each of which is within 1 km radius of the city-district weather station. Furthermore, considering that the AMIS only started in 2010, going through the system testing period 2010-2013, 2012-14 were selected as the temporal scope for the AMIS energy (electricity) bill data. Finally, the locations of the 98 apartment neighbourhood (AN) sites together with the 19 city-district weather station sites selected for the relational study are identified (Figure1).

2.2.3. Property price data

The AMIS data portal also provides apartment property price data by linking to the information service of publicly noticed value (PNV) of real estate price (KAB, 2015), which is maintained by the Korea Appraisal Board (KAB, 2017) under the MoLIT. Therefore, the apartment property price data in this study is not of market price, but of PNV for calculating household's property tax. Like energy use data, the unit of the property price is Korean Won per square metre (KRW/m^2) and the time period to collect was 2012-14.

2.2.4. Seoul's climate change projection data

Established by the Korea Meteorological Administration (KMA), the Climate Information Portal (CIP) provides climate change datasets projected by MK-PRISM (Modified Korean Parameter-elevation Regressions an Independent Slopes Model) (CIP, 2017; Kim et al., 2012; Kim et al., 2013a). The publicly available dataset contains daily maximum, minimum and mean temperature and precipitation data up to Year 2100 at the city-district level. The MK-PRISM model was developed based on the historical weather dataset of each CD-AWS between 2001 and 2010 with 1 km horizontal resolutions, including topographic effect and data histogram. The climate change scenarios used in this projection were RCP (Representative Concentration Pathways) based, reflecting the recent trend of CO_2 concentration change corresponding to global responses to climate change. There are four scenarios: RCP 2.6, 4.5, 6.0, 8.5 with the CO_2 concentration reaching 420, 540, 670 and 940 ppm in 2100 respectively. Of the four scenarios, RCP 4.5 and 8.5 were selected for this study. Also, the daily mean temperature data was collected for each city district in Seoul to generate future summer monthly average temperatures.

3. Methodology

3.1 Data mining

Our initial survey of the above open datasets from the 19 city districts suggests a need for a systematic approach to analysing the data in relation to our research question. Hence, we developed a data mining method in three steps: extracting summer cooling energy use data, identifying the summer cooling period and data normalisation.

Firstly, in searching for potential correlations between energy use (electricity bill) and urban weather data (air temperature etc.), it is necessary to minimize inclusion of the non-weather-dependent electricity bill (Asimakopoulos et al., 2001). In our study, the increasing rate (IR) of monthly electricity bill during summer period was proposed as a cooling energy use index which can be calculated by the increment of electricity bill of each summer month based on the non-weather-dependent electricity bill of the year. The non-weather-dependent bill can be identified as the minimum electricity bill of the year, because it shows the operating costs of lighting and home appliances not affected by the external thermal conditions (Bronson et al., 1992). The equation for calculating the monthly IR of an apartment neighbourhood is simply as follows (Equation 1), where B_{sm} is the summer monthly electricity bill and B_{min} is the non-weather-dependent electricity bill:

$$IR\ (\%) = \frac{(B_{sm} - B_{min})}{B_{min}} \times 100 \qquad (1)$$

It may be debatable whether the minimum electricity month excludes any cooling and heating energy use or not. In reality, it is difficult to be sure of this differentiation due to the complexity of user behaviour and circumstances in residential energy use. Here we assumed that the month where the minimum electricity bill occurs was non-weather-dependent or, at least, it was minimal in cooling and heating energy use. Figure 2 supports this assumption, showing that monthly temperature distribution and the monthly IR in 2012 as an example. For Seoul, the base temperature for HDD and CDD was determined at 17.1°C as a transition point of electricity demand from heating to cooling (Lee et al., 2014). As seen in monthly temperature distribution, May and October are placed on near the base temperature and therefore, about 60% of 98 ANs showed that the minimum electricity bill occurred in May (28%) and October (29%). Moreover, the minimum IR occurred in both months (about 60% of ANs), only 4.67% and 5.06% respectively.

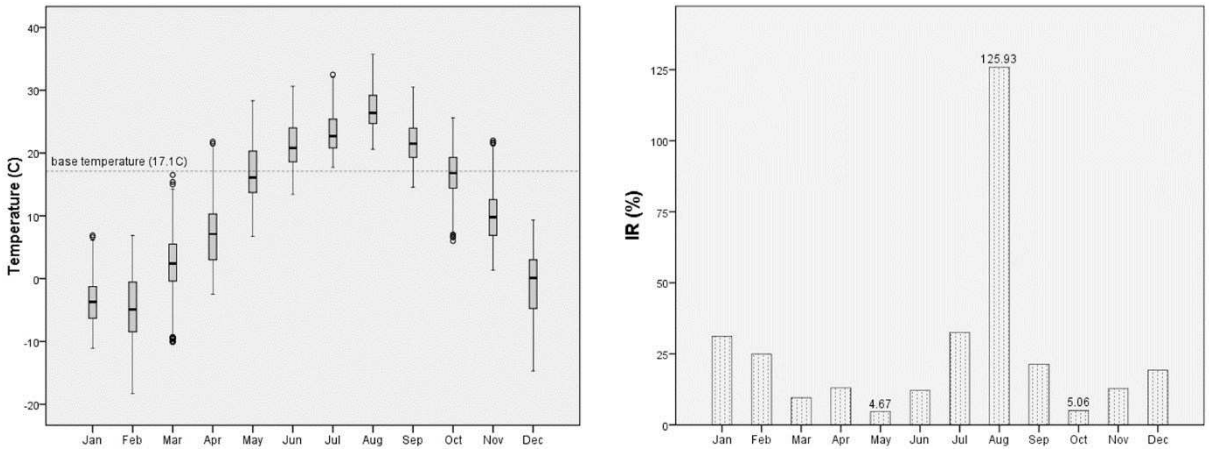

Figure 2. Monthly temperature distribution based on hourly dataset from city weather station for 2012 (left) and monthly IR data of aggregate of all 98 ANs across the 19 CD's boundaries (right).

Secondly, the summer cooling period in Seoul was identified by the monthly IR distribution. The Korean Meteorological Administration (KMA) currently stipulates June, July and August as the official summer months (KMA, 2014). However, we propose to review the summer months in Seoul according to the distribution of the IRs during May and September 2012-2014. The distribution of the monthly IRs was calculated as the mean of monthly IR of all apartment neighbourhoods in Seoul. Notably, the time frame (day) in the IR-based analysis is set to the metre reading day of electricity billing: the 18th of each month, which is also applied to the city-district weather station datasets. Through our monthly IR distribution analysis, July-September was identified as the summer cooling period in Seoul 2012-14, which was applied to the corresponding AWS datasets.

Finally, as the main statistical approach of this study would be parametric statistics (e.g. Pearson correlation and analysis of variance), normality of the IR values was checked first. Also, it was carried out by each summer month (July, August, and September) during 2012-2014 due to the monthly time base of each parametric analysis. The output of normality distribution of the IR is shown in Table 2.

The normality of July and August IR was reasonably accepted as each value of skewness (the symmetry of the distribution) and Kurtosis (the 'peakedness' of the distribution) was less than 1. However, as the September IR and the Summer Period IR did not meet normality condition, which skewness and Kurtosis were 1.898 (1.484) and 5.301 (2.299) respectively, the IR data was transformed using square root (Sqrt) transformation recommended by Tabachnick and Fidell (2007). Considering coherence of data transformation, all IR data was therefore Sqrt transformed. Figure 3 shows the normality distribution of original (left) and Sqrt transformed (right), taking the September IR as an example.

Table 2. Normality distribution of IR (increase rate of energy use for cooling) of the 98 apartment neighbourhoods (ANs) by each of the summer months and the summer period 2012-2014. Values in () are square root transformed IR

	N	Mean	Std. D	Skewness	Kurtosis	Kolmogorov-Smirnov Sig.
Jul IR	294	37.94	23.62	.942	.508	.000
	(98ANs x 1mon x 3yr)	(5.86)	(1.90)	(.270)	(-.449)	(.077)
Aug IR	294	96.02	48.77	.803	.446	.002
	(98ANs x 1mon x 3yr)	(9.49)	(2.46)	(.254)	(-.519)	(.004)
Sept IR	294	24.43	20.67	1.898	5.301	.000
	(98ANs x 1mon x 3yr)	(4.44)	(2.17)	(-.015)	(.662)	(.000)
Summer Period	882	52.80	45.65	1.484	2.299	.000
IR (Jul–Sept)	(98ANs x 3mon x 3yr)	(6.60)	(3.05)	(.393)	(.017)	(.000)

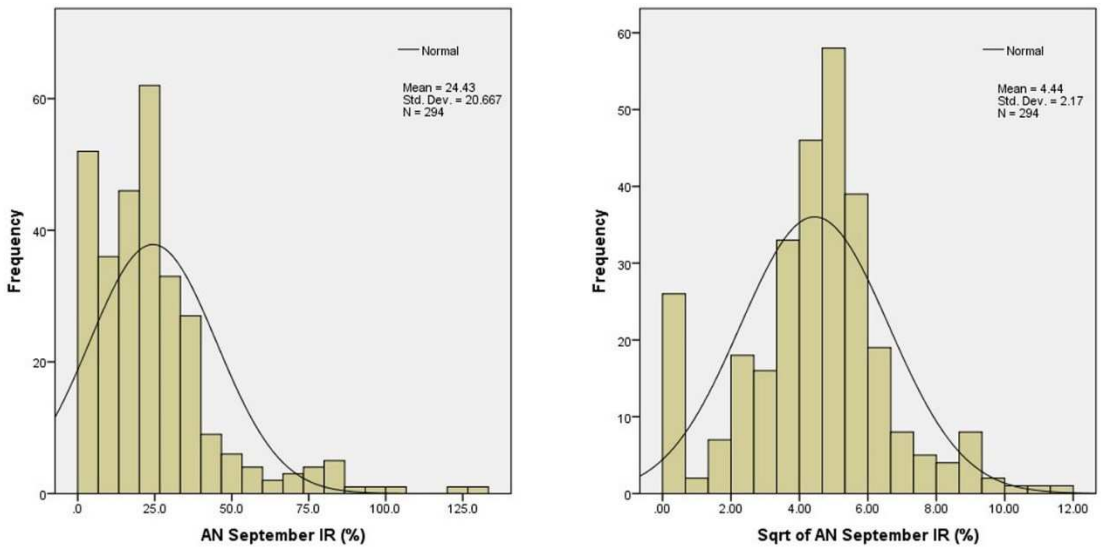

Figure 3. Normality distribution of original (left) and Sqrt transformed (right) September IR of the 98 apartment neighbourhoods (ANs).

3.2. A statistic relational analysis framework

To analyse the open data consistently, we develop a statistic relational analysis framework and the workflow for correlating cooling energy use with urban microclimate and property price data (Figure 4). Here we conduct statistic relational studies at two spatial scales: (a) at the macro-level, aggregating the 98 apartment neighbourhoods (ANs) within the AWS 1km boundaries across the 19 city districts, and (b) at the micro-level, aggregating only the ANs within each CD-AWS 1km boundary individually. The results from the correlational analyses provide a basis for projecting future summer peak energy demands given the climate change projections made available at the city-district level.

Firstly, at a macro-level, for the 98 apartment neighbourhoods (AN) drawn from the 19 CDs' AWS 1km boundaries, the relationships between cooling energy use (IR) and the two variables (urban weather and property price data) were explored by Pearson correlation analyses (RA1, RA2). Then, a multiple linear regression analysis was done to compare the impact of the two variables on IR (RA3).

Secondly, at a micro-level, moving into each CD's AWS 1km boundary individually, the number of apartment neighbourhoods varies from 3 to 10, the relationships between cooling energy use and urban weather data were examined in two aspects: (1) The diversity of IR by analysis of variance (SA1); (2) the relationship between IR and AWS data by Pearson correlation (RA4). Then, due to the varying strength of correlation in summer months and exceptionally strong correlation coefficients found in August (the hottest month of the

year), a simple bivariate regression (SBR) model was derived for each of the 19 city district AWS boundaries (RA5). The SBR models were evaluated by residual analysis (SA2). Finally, the SBR models were applied to estimate future peak energy demands of each city district using the climate change projection data for South Korea.

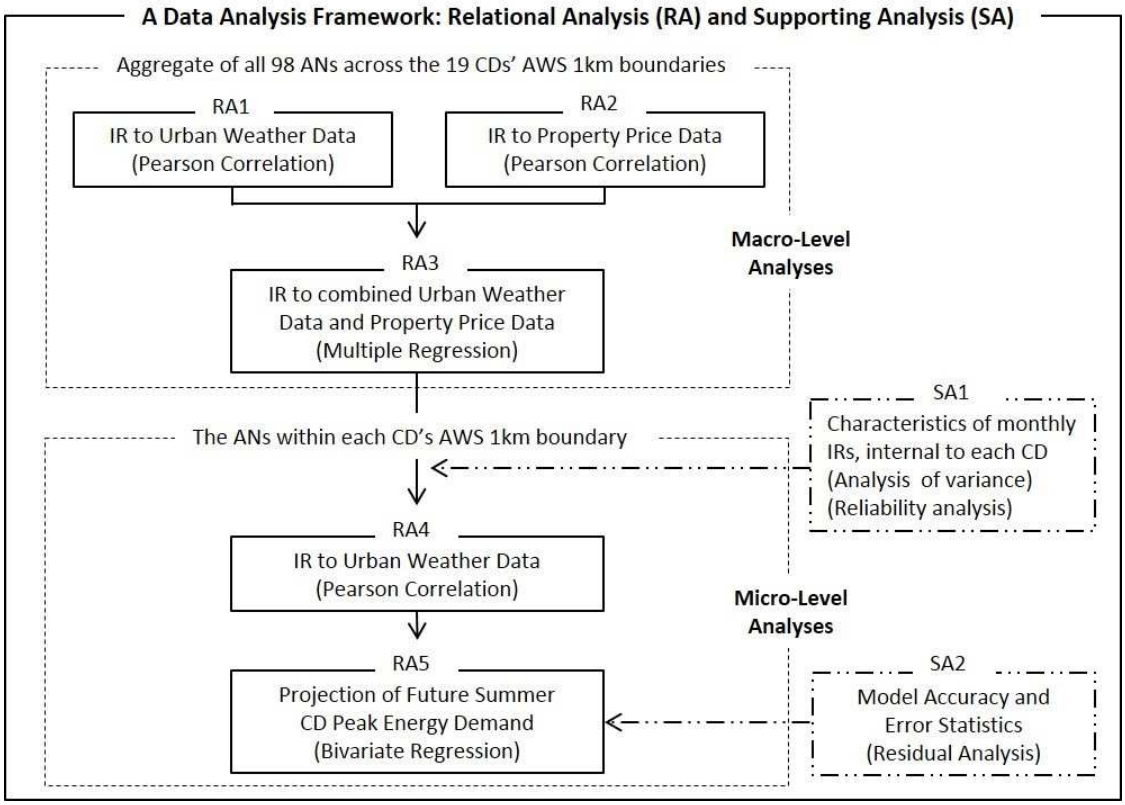

Figure 4. A statistic relational analysis framework for correlating cooling energy use with urban weather and property price data as a basis for projecting future summer peak energy demand.

4. Results and discussion

4.1. Correlating cooling energy use with air temperature (RA1)

The relationship between the cooling energy use (Sqrt IR) and the urban weather (monthly average temperature) of the 98 apartment neighbourhoods within the 19 CDs' AWS 1km boundaries was examined by Pearson correlation analyses. To confirm no violation of the assumption of normality, linearity and homoscedasticity, a preliminary analysis was carried out for the whole summer period, and July, August and September of 2012-2014 (Figure 5).

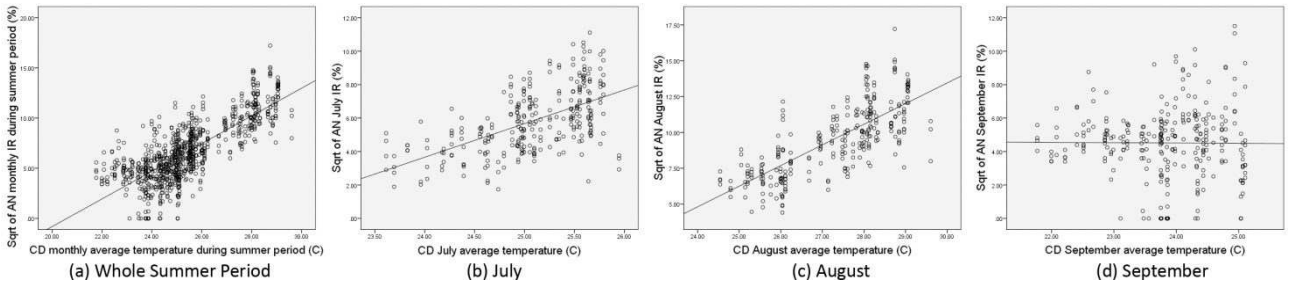

Figure 5. Scatterplot between cooling energy use (Sqrt IR) and monthly average temperature.

Table 3 shows that there was a very strong and positive correlation between the two variables for the whole summer period (r=.770). For individual months, July (r=.574) and August (r=.749) show strong or very strong positive correlations but September (r=-0.009) shows negative, no correlation and no significance.

Table 3. Correlation between cooling energy use (Sqrt IR) and monthly average temperature. (** p<0.01; * p <0.05)

		Sqrt of AN monthly IR (Whole Summer)	Sqrt of AN monthly IR (July)	Sqrt of AN monthly IR (August)	Sqrt of AN monthly IR (September)
monthly average temperature	Pearson-C	.770**	.574**	.749**	-.009
	Sig.	.000	.000	.000	.882
	r squared	.593	.329	.561	.000
	N	882 (98ANs*3Mon*3Yr)	294 (98ANs*1Mon*3Yr)	294 (98ANs*1Mon*3Yr)	294 (98ANs*1Mon*3Yr)

To explore what might have contributed to the differences in the Pearson correlation coefficients seen in Table 3, we looked into another possible urban weather parameter—changes in humidity. However, as no humidity data available at the AWS portal, the monthly temperatures were grouped into 2 types: monthly average temperature during Precipitation and Non-precipitation days (Table 4). It could be debatable if the humidity change can be simplified in those two temperature types. However, under the complexity of urban weather and limited data availability, it is assumed that the humidity condition in non-precipitation days is definitely drier than in precipitation days.

Firstly, the cooling energy use over the whole summer period (N=882, 98ANs*3Mon*3Yr) had a stronger correlation with non-precipitation average temperature (r=.762) than precipitation (r=.738), implying that air temperatures in non-precipitation days may have been more influential on residential cooling energy use. This was also confirmed in the monthly correlation analysis: in July and August (N=294, 98ANs*1Mon*3Yr), the non-precipitation average temperature was more strongly correlated with IR than precipitation. Secondly,

comparing the two correlations in Table 3 and Table 4, the cooling energy use was more strongly correlated with monthly average temperature in all summer months. Therefore, our relational study was carried out using only the monthly average temperature. However, the September case still showed no correlation, suggesting that under the mildest summer condition, other parameters such as solar radiation may be more influential than temperature.

Table 4. Correlation between cooling energy use (Sqrt IR) and monthly average temperature in precipitation and non-precipitation days. **. p <0.01 and *. p <0.05

		Sqrt of AN monthly IR (Whole Summer)	Sqrt of AN monthly IR (July)	Sqrt of AN monthly IR (August)	Sqrt of AN monthly IR (September)
Precipitation monthly average temperature	Pearson-C	.738**	.443**	.693**	.027
	Sig.	.000	.000	.000	.647
	r squared	.545	.196	.481	.001
	N	882 (98ANs*3Mon*3Yr)	294 (98ANs*1Mon*3Yr)	294 (98ANs*1Mon*3Yr)	294 (98ANs*1Mon*3Yr)
Non-Precipitation monthly average temperature	Pearson-C	.762**	.525**	.746**	-.059
	Sig.	.000	.000	.000	.317
	r squared	.580	.276	.556	.003
	N	882 (98ANs*3Mon*3Yr)	294 (98ANs*1Mon*3Yr)	294 (98ANs*1Mon*3Yr)	294 (98ANs*1Mon*3Yr)

4.2. Correlating cooling energy use with apartment property price data (RA2)

To account for possible human behavioural factors of cooling energy use (i.e., factors associated with decision on using cooling energy or not and how much), we investigated if cooling energy use was correlated to apartment property price data. Here, we assume that the apartment property price is an overall indicator of the socio-economic circumstances of households, affecting residents' cooling energy use decisions. Since the property price data was published as the average price of 2012-2014, the correlation analysis was carried out based on total cooling energy use (IR) of the whole summer period and each summer month during 2012-2014; thus, the number of items in all cases was 98. The property price data was also Sqrt transformed for data normalization.

Table 5. Correlation between cooling energy use (Sqrt IR) and Sqrt of property price 2012-2014. **. p<0.01

		Sqrt of total AN monthly IR (Whole Summer Period)	Sqrt of total AN monthly IR (July)	Sqrt of total AN monthly IR (August)	Sqrt of total AN monthly IR (September)
Sqrt of AN property price	Pearson-C	.712**	.698**	.708**	.101
	Sig.	.000	.000	.000	.324
	R-squared	.507	.487	.501	.010
	N	98	98	98	98

Table 5 shows that the two variables had positive and very strong coefficient during whole summer period (r=.712). However, the strength of the monthly coefficient varied, July (r=.698), August (r=.708), September (r=.101), suggesting higher cooling energy use correlated with higher apartment property prices. Interestingly, comparing the two correlations in Table 3 and Table 5, the July correlation coefficient of property price (r=.698) was much stronger than that of average temperature (r=.574). This could imply that under milder weather conditions (July in this case), the socio-economic factor, as reflected in the apartment property price data, can be more influential than the external weather conditions on cooling energy use. To explore this further, a multiple regression analysis was conducted to investigate the combined effect of urban weather data and property price data on cooling energy use in the next section.

4.3. Effect of combined air temperature and property price on cooling energy use (RA3)

Firstly, the multi-collinearity was assessed using tolerance and VIF (Variance inflation factor) in collinearity statistics. The tolerance and VIF in 4 cases were not less than .10 and not above 10 respectively, so the multi-collinearity assumption was not violated: whole summer period (.969 and 1.032), July (.751 and 1.332), August (.951 and 1.052) and September (.820 and 1.220). Furthermore, a preliminary analysis for regression model was carried out to check outliers, normality, linearity, homoscedasticity and independence of residuals through inspecting the normal probability plot (P-P) of the regression standardised residual and the scatterplot.

Table 6. Multiple regression analyses to investigate effect of combined monthly average temperature and Sqrt of property price on cooling energy use (Sqrt IR)

Case regression model	Dependent	Independent	*B*	Std. error	Beta	*p* value
Whole Summer Period	Sqrt of AN monthly IR for whole summer months	(Constant)	-29.656	.973		.000
		Monthly average temperature	1.332	.038	.744	.000
R^2 = .613, *p* = .000		Sqrt of AN property price	.001	.000	.146	.000
July	Sqrt of AN monthly IR for July	(Constant)	-28.245	3.964		.000
		July average temperature	1.162	.167	.331	.000
R^2 = .506, *p* = .000		Sqrt of AN property price	.002	.000	.485	.000
August	Sqrt of AN monthly IR for August	(Constant)	-30.282	1.808		.000
		August average temperature	1.304	.068	.679	.000
R^2 = .655, *p* = .000		Sqrt of AN property price	.002	.000	.314	.000
September	Sqrt of AN monthly IR for September	(Constant)	6.422	3.839		.095
		September average temperature	-.129	.172	-.048	.453
R^2 = .007, *p* = .224		Sqrt of AN property price	.001	.000	.094	.147

Table 6 shows the result from the regression analysis. Firstly, the regression model explained 61.3%, 50.6% and 65.5% of the variance in the Sqrt of neighbourhood monthly IR for whole summer period, July, and August 2012-2014 respectively; the statistical significance in all 3 models was .000 ($p<.0005$). Secondly, evaluating each of the independent variables, the impact of each variable on cooling energy use was different. In the whole summer period model, the impact of microclimate temperature (Beta, .744) on cooling energy use was much higher than the property price (.146). However, comparing the Beta values between July and August, while the impact of average property price (.485) was higher than that of monthly average temperature (.331) in July, the temperature (.679) was more influential on cooling energy use than the price (.314) in August. This suggests that under the high temperature of August, the influence of weather condition on cooling energy use is more dominant than that of the socio-economical (as reflected by the property price). But under the lower temperature of July, the socio-economic factor appears more dominant.

4.4. Correlating cooling energy use with air temperature within each CD's AWS 1km boundary (RA4)

Following the three relational analyses above at the macro-level (RA1-RA3 in Figure 4), we performed two further analyses at the micro-level (RA4, RA5), looking into the apartment neighbourhoods within each city district's AWS 1km boundary.

4.4.1. Characteristics of monthly IR for cooling energy use (SA1)

Figure 6 shows the August average air temperatures (19 Jul – 18 Aug, 2012) recorded at each city district AWS in Seoul, the hottest period during 2012-2014. The highest average August cooling energy use appeared also in 2012. However, in that period the average temperatures varied, and the gap between the highest and lowest was about 2.65^{o}C (the highest 29.61^{o}C occurred at CD25, while the lowest 26.96^{o}C at CD22). Moreover, some city district temperatures differed significantly from the Seoul City Weather Station temperature (28.21^{o}C). Secondly, the August IR for cooling energy use also shows noticeable variations across the 19 city districts. Thirdly, these two measurements are not always in agreement with our intuition that higher air temperatures correspond to higher IRs and vice versa. As shown by the macro analyses above, socio-economic factor (reflected in the property price) could also affect cooling energy use significantly. For instance, CD25 is an example: low IR, high temperature, and low property price band. The highest IR occurred at CD21 (high temperature, high property price band), while the lowest IR occurred at CD17 (low temperature, low property price band).

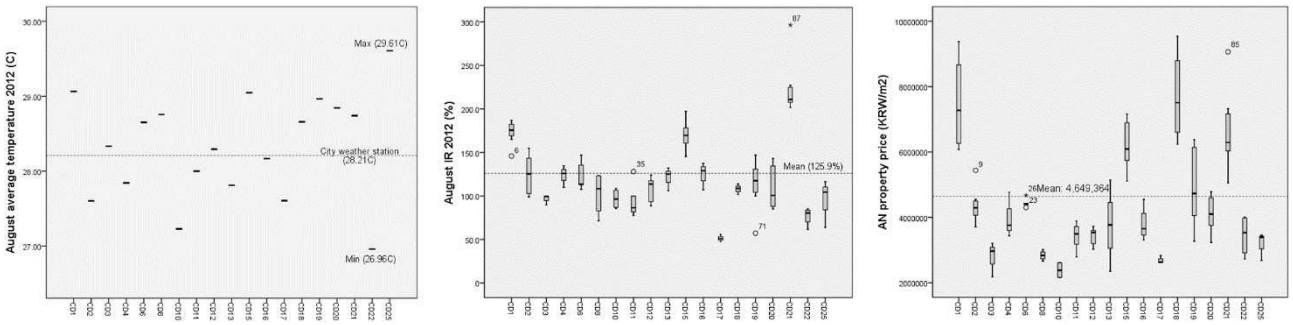

Figure 6. The August average temperature (left) and August ANs' IR (middle) in 2012, and AN's property price (right) within each of the 19 CDs' AWS 1km boundary.

The difference in cooling energy use across the 19 CDs was explored by a one-way between-groups analysis of variance (ANOVA). As the climate conditions of each summer month were different, the ANOVA was carried out monthly for July, August, and September, 2012-2014. The ANOVA result in Table 7 shows that the difference in the monthly IR of the 19 CDs is statistically significant ($p < 0.05$).

Table 7. Analysis of variance (ANOVA) of monthly IR of July, August and September, 2012-2014, across the 19 city districts

	F	Sig. (*p*)
Sqrt July IR	26.308	.000
Sqrt August IR	9.285	.000
Sqrt September IR	14.708	.000

Moreover, we observe that there appears a close similarity of monthly IR distribution within each CD boundary. Their internal consistency and the similarity was examined using Cronbach's Alpha and correlation coefficients between inter-items (monthly IR of each AN) respectively. As seen in Table 8, the Cronbach's alpha coefficients in all CDs were above 0.9 except CD17, but even CD17 was above 0.8. Furthermore, the average of correlation coefficients between inter-items was above 0.7 in all cases. This means high internal consistency and similarity in terms of the distribution of monthly cooling energy use within each CD-AWS 1km boundary. Therefore, it is reasonable to assume that the apartment buildings are mostly surrounded with homogeneous microclimatic conditions, especially air temperatures.

Table 8. Cronbach's alpha coefficients and correlation coefficients between inter-items of monthly cooling energy use (IR) in each city district's AWS 1km boundary: () standardised Cronbach's alpha

	Cronbach's alpha coefficients	Correlation coefficients between inter-items (N=9, Jul to Sep 2012-14)						Number of ANs
		Avg	Min	Max	Range	Max/Min	variance	
CD1	.982 (.985)	.893	.741	.996	.255	1.344	.007	8
CD2	.986 (.992)	.945	.876	.994	.118	1.135	.001	7
CD3	.948 (.949)	.860	.742	.922	.180	1.243	.008	3
CD4	.990 (.993)	.978	.960	.992	.032	1.034	.000	3
CD6	.989 (.995)	.977	.952	.991	.038	1.040	.000	5
CD8	.922 (.941)	.799	.554	.962	.408	1.737	.018	4
CD10	.992 (.993)	.973	.959	.998	.039	1.041	.000	4
CD11	.953 (.968)	.860	.693	.953	.260	1.375	.008	5
CD12	.985 (.991)	.958	.912	.975	.063	1.069	.000	5
CD13	.974 (.978)	.936	.890	.991	.101	1.114	.002	3
CD15	.984 (.985)	.892	.638	.997	.359	1.562	.011	8
CD16	.986 (.990)	.961	.931	.989	.058	1.062	.001	4
CD17	.839 (.880)	.710	.453	.916	.462	2.022	.044	3
CD18	.965 (.972)	.896	.779	.981	.202	1.260	.008	4
CD19	.990 (.994)	.946	.737	.999	.262	1.355	.003	10
CD20	.990 (.993)	.946	.810	.996	.186	1.230	.003	8
CD21	.988 (.989)	.928	.828	.995	.167	1.202	.003	7
CD22	.959 (.960)	.857	.731	.984	.253	1.345	.007	4
CD25	.947 (.974)	.927	.882	.962	.080	1.090	.001	3

4.4.2. Apartment building information

Holistically speaking, energy use for cooling in the context of this study can be characterised as a human comfort and economic decision in response to the result of dynamic interaction between building envelope and surrounding urban microclimate. The variation or similarity of physical thermal properties of the apartment buildings play a certain role in the characteristics of cooling energy use seen at the city district level. However, here we adopt an "all in the energy bill" approach as a wrapper encompassing some aspects of the complex physical interactions. Nonetheless, some key building information is presented in this subsection. We first collated the building insulation criteria (U-value) according to the year of building regulation applied. Figure 7 (left) shows that there is one dominant insulation regulation type in each CD boundary although some CDs are mixed (e.g. CD8 & 15). However, even those 2 CDs can be grouped into one dominant insulation type because the adjacent insulation criteria have similarity in terms of the U-value (see Table 9). Secondly, as seen in Figure 7 (right), there appears one dominant size of apartment total floor area in each CD, representing similarity of the household size.

Thirdly, an apartment building's glazing ratio and its orientation can affect its internal solar gain to a large extent. However, the cost of collecting such detailed building information is prohibitive given the large sample size (72,104 apartment buildings in total). Here we referred to a previous study on glazing ratio (Kim et al.,

2010). We assume that the 98 ANs may have similar glazing ratios (Table 10). However, given this limited information, the characteristic of glazing ratio within each CD boundary remains inconclusive.

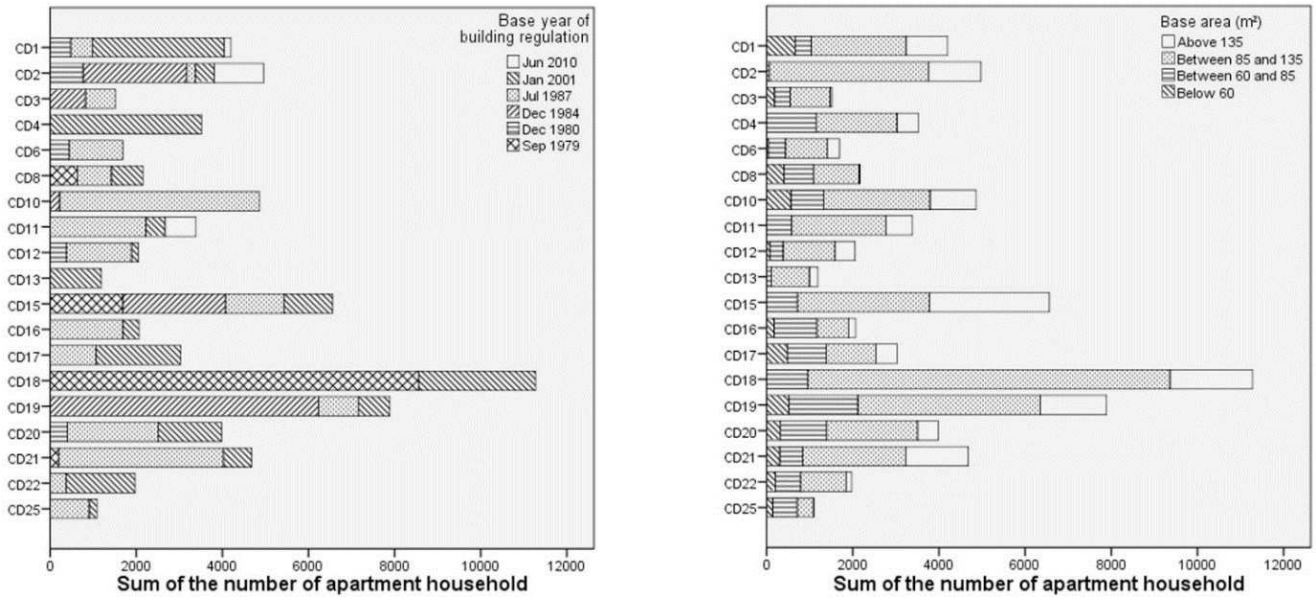

Figure 7. The number of apartment households (units) within each CD-AWS boundary according to the building insulation criteria applied in certain built years (left) and the ranges of floor area (right).

Table 9. U-value of insulation criteria for Seoul by base-year's building regulation (W/m^2*K). (Source from Kim et al., 2013b) * Side wall represents the external wall without opening area, such as glazing

Base year	External wall	External/ Ground Floor	External Roof	Side wall	Window
Sep 1979	1.05	1.05	1.05	-	2.56
Dec 1980	.58	1.16	.58	-	3.49
Dec 1984	.58	.58	.58	.47	3.49
Jul 1987	.58	.58	.41	.47	3.37
Jan 2001	.47	.35	.29	.35	3.84
Nov 2008	.47	.35	.29	.35	3.0
Jun 2010	.36	.30	.20	.27	2.1

Table 10. Average glazing ratio (%) of the apartment building by type of apartment building. (Source from Kim et al., 2010)

Faced orientation	Tower type	Flat type	Total (Tower +Flat)
South	61.48	34.98	41.91
East	48.57	22.00	28.80
West	70.19	25.65	36.10
North	56.49	46.30	49.48

4.4.3. Correlating cooling energy use with air temperature within each CD-AWS 1km boundary

Given the unique characteristics and internal consistency of monthly cooling energy use in each CD, a relational study between cooling energy use (Sqrt IR) and urban weather data was carried out within each CD-AWS 1km boundary. Shown in Table 11, for the whole summer period, there were positive and very strong correlation coefficients between Sqrt IR and monthly average air temperature in most CDs (r>.700 and even r>.900 in some cases). However, several city districts stand out with relatively smaller correlation coefficients (r<.700), for instance, CD11, CD13, CD17 and CD22.

Table 11. Correlation between cooling energy use (Sqrt IR) and monthly average temperature. (** p<0.01; * p <0.05) within each CD-AWS 1km boundary. **. p<0.01 and *. p<0.05

	Whole summer months (Jul – Sept inclusive)			**July**		**August**		**September**		
	Pears-C	Sig.	N	Pears-C	Sig.	Pears-C	Sig.	Pears-C	Sig.	N
CD1	.883**	.000	72, 8ANs	.306	.146	.913**	.000	.143	.504	24, 8ANs
CD2	.890**	.000	63, 7ANs	.523*	.015	.877**	.000	-.114	.624	21, 7ANs
CD3	.850**	.000	27, 3ANs	.323	.397	.959**	.000	.043	.912	9, 3ANs
CD4	.909**	.000	27, 3ANs	.863**	.003	.937**	.000	.001	.997	9, 3ANs
CD6	.928**	.000	45, 5ANs	.691**	.004	.918**	.000	.100	.723	15, 5ANs
CD8	.819**	.000	36, 4ANs	-.055	.865	.836**	.001	.118	.716	12, 4ANs
CD10	.942**	.000	36, 4ANs	.742**	.006	.972**	.000	.069	.831	12, 4ANs
CD11	.628**	.000	45, 5ANs	.509	.052	.738**	.002	-.088	.755	15, 5ANs
CD12	.891**	.000	45, 5ANs	.552*	.033	.943**	.000	.006	.984	15, 5ANs
CD13	.649**	.000	27, 3ANs	.869**	.002	.870**	.002	-.084	.830	9, 3ANs
CD15	.881**	.000	72, 8ANs	.283	.180	.931**	.000	.415*	.043	24, 8ANs
CD16	.932**	.000	36, 4ANs	.802**	.002	.948**	.000	.385	.217	12, 4ANs
CD17	.267	.178	27, 3ANs	-.282	.462	.684*	.042	-.432	.246	9, 3ANs
CD18	.896**	.000	36, 4ANs	.263	.408	.960**	.000	.401	.196	12, 4ANs
CD19	.848**	.000	90, 10ANs	-.136	.475	.838**	.000	.702**	.000	30, 10ANs
CD20	.829**	.000	72, 8ANs	-.339	.106	.909**	.000	.213	.317	24, 8ANs
CD21	.898**	.000	63, 7ANs	.696**	.000	.883**	.000	-.210	.361	21, 7ANs
CD22	.616**	.000	36, 4ANs	-.045	.890	.726**	.007	.004	.990	12, 4ANs
CD25	.739**	.000	27, 3ANs	-.861**	.003	.774*	.014	-.328	.388	9, 3ANs

Among the monthly correlation coefficients, the August correlations were the strongest and most consistent, while July varied and September were the weakest, showing no relation or even negative. Moreover, the August coefficients increased dramatically even in the aforementioned four districts, compared to whole summer correlation coefficients. This suggests that under extreme weather conditions, such as August (being the hottest month in Seoul), the external temperature can be the key parameter in affecting residential cooling energy use in most CDs. On the other hand, under relatively milder weather conditions (i.e. July or September), there may be other parameters affecting cooling energy use.

The results of the monthly correlation coefficients found at the micro-level are similar to those found at the macro-level (see section 4.1, Table 3): August (strongest, r=.749); July (strong, r=.574); September (negative and no correlation, r=-.009). However, seen at the micro-level, the strength of correlation coefficients varies among the CDs. We see that there are not only temporal variations in relationship between residential cooling energy use and urban microclimate data, but also spatial variations.

4.4.4. Other parameters affecting residential cooling energy use

Why did the 4 CDs (CD11, CD13, CD17 and CD22) show relatively smaller correlation coefficients (Table 11)? Firstly, common to these CDs is a relatively small sample size (3 to 5 ANs). As the statistical approaches used in this study are parametric, the output can be sensitive to sample size. For example, the internal consistency and the correlation coefficients between inter-items of those 4 CDs are relatively small (see Table 8), especially, the minimal coefficient in CD17 was only .453. With a small sample size, such a weak internal consistency could result in a weak relationship.

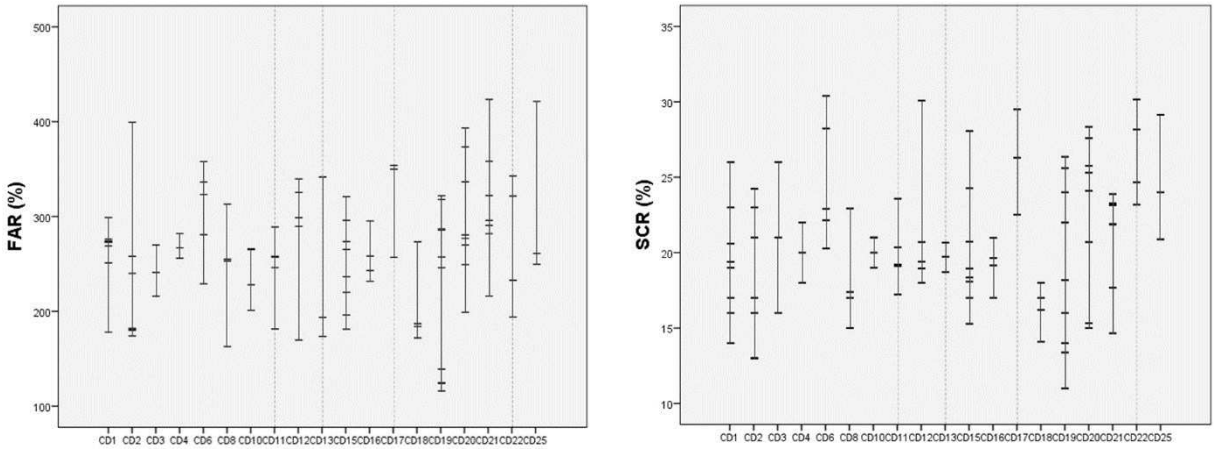

Figure 8. The actually applied floor area ratio (FAR, left) and site coverage ratio (SCR, right) of ANs within each CD-AWS boundary.

Secondly, there may be other variables (e.g. solar radiation) affecting cooling energy use in such CDs. As recent studies show that air temperature and solar radiation play a key role in residential cooling energy use at the same time (Flor & Domınguez, 2004; Salvati et al., 2017), we investigated the probability of solar radiation impacts on these 4 CDs, through analysing floor area ratio (FAR) and site coverage ratio (SCR) as a density indicator (Figure 8). Here both the FAR and SCR are the percentage ratios actually applied in the 98 existing ANs, not inferred from the building regulation of land use. Interestingly, there appears characteristics

in the FAR of the four CDs: one or two ANs had exceptionally different FAR values. The different density may affect different internal solar gains and in turn, lead to different cooling energy use, resulting in weak internal consistency, and finally, it results in smaller correlation coefficients within a small sample size. However, the SCR plot is inconclusive. This implies that those four CDs, showing relatively weaker correlation coefficients, may need to take solar radiation into account in correlating cooling energy use. Finally, there may be socio-economic factors (e.g. property price) common to these CDs that belong to a relatively lower property price band (see Figure 6, right). Here the socio-economic factor as represented by property price may be more influential than the external temperature even in August.

4.5. Estimating future peak cooling energy demands (RA5)

Given the result from the Pearson correlation analysis of IR to monthly average temperature (RA4), which was corroborated by ANOVA and Cronbach's alpha coefficients analyses (SA1), we derive city-district specific models for estimating future peak cooling energy demands according to the latest climate change projection for Seoul. This is achieved by a bivariate regress analysis (RA5, section 4.5.1) checked by model accuracy and error statistics (SA2, section 4.5.2). The peak demand estimations for each city district are then presented in section 4.5.3.

4.5.1 Simple bivariate regression (SBR) models

As the cooling energy use (IR) shows strong correlation with the external temperature in August, a simple cooling energy use model for estimating peak cooling demand for each CD boundary can be derived from bivariate regression. The purpose of this modelling exercise is to estimate cooling energy use for each city district (within the AWS 1 km boundary), not for an individual apartment neighbourhood. Hence, the dependent variable (Sqrt IR) should be the sum or an average of all ANs' IR within each CD boundary as its peak cooling energy use. However, due to the small sample size (N=3, 2012-2014 August) imposed by the limited time period of the current AMIS data availability, an alternative was considered. As seen in section 4.4.1, the characteristic of ANs IR data shows that there is very good internal consistency and similarity in terms of the distribution of monthly cooling energy use (Sqrt IR) within each CD boundary. Based on these findings, the Sqrt IR of individual ANs within each CD boundary was used as a dependent variable. A preliminary bivariate regression analysis was carried out to check outliers, normality, linearity, homoscedasticity and independence of residuals through inspecting the normal probability plot (P-P) of the regression standardised residual and the scatterplot for each CD. The resultant 19 SBR models are presented in Table 12.

Table 12. Simple bivariate regression (SBR) models for estimating each CD's peak cooling demand within its AWS 1km boundary

Sqrt of AN Aug IR of	Constant		CD Aug average temp						
	B	*p* value	*B*	*p* value	R	R^2	Adjusted R^2	Sig.	N
CD1	-30.126	.000	1.505	.000	.913	.834	.827	.000	24 (8 ANs)
CD2	-34.159	.000	1.632	.000	.877	.769	.757	.000	21 (7 ANs)
CD3	-27.637	.000	1.315	.000	.959	.919	.908	.000	9 (3 ANs)
CD4	-31.872	.001	1.526	.000	.937	.878	.860	.000	9 (3 ANs)
CD6	-31.228	.000	1.466	.000	.918	.843	.831	.000	15 (5 ANs)
CD8	-23.132	.005	1.148	.001	.836	.699	.669	.001	12 (4 ANs)
CD10	-33.680	.000	1.603	.000	.972	.945	.940	.000	12 (4 ANs)
CD11	-18.437	.017	.985	.002	.738	.544	.509	.002	15 (5 ANs)
CD12	-31.226	.000	1.463	.000	.943	.889	.880	.000	15 (5 ANs)
CD13	-14.240	.027	.895	.002	.870	.756	.722	.002	9 (3 ANs)
CD15	-39.766	.000	1.828	.000	.931	.867	.861	.000	24 (8 ANs)
CD16	-28.738	.000	1.427	.000	.948	.899	.888	.000	12 (4 ANs)
CD17	-3.229	.439	.367	.042	.684	.468	.392	.042	9 (3 ANs)
CD18	-34.153	.000	1.564	.000	.960	.921	.913	.000	12 (4 ANs)
CD19	-34.035	.000	1.563	.000	.838	.702	.691	.000	30 (10 ANs)
CD20	-42.146	.000	1.838	.000	.909	.826	.818	.000	24 (8 ANs)
CD21	-35.252	.000	1.749	.000	.883	.780	.769	.000	21 (7 ANs)
CD22	-9.425	.096	.657	.007	.726	.527	.480	.007	12 (4 ANs)
CD25	-17.332	.067	.926	.014	.774	.599	.541	.014	9 (3 ANs)

4.5.2. Model accuracy and error statistics (SA2)

To evaluate the SBR model accuracy, error statistics between predicted and observed CD cooling energy use was calculated. The SBR model was derived from ANs' IR data within each CD boundary for August 2012-14 as the training data; the Sqrt of average ANs' IR within each CD boundary for August 2015 (provided by the AMIS) was used as the testing data. We calculated five criteria using the following equations, where y_i is the predicted and y_i' is the observed: mean absolute error (MAE); mean square error (MSE); root mean square error (RMSE); mean absolute percentage error (MAPE); coefficient of determination (R^2) (Catalina et al., 2013).

$$MAE = \frac{\sum_{i=1}^{n} |y_i - y_i'|}{n} \quad (2)$$

$$MSE = \frac{\sum_{i=1}^{n} (y_i - y_i')^2}{n} \quad (3)$$

$$RMSE = \sqrt{\frac{\sum_{i=1}^{n} (y_i - y_i')^2}{n}} \quad (4)$$

$$MAPE = \frac{\sum_{i=1}^{n} \left| \frac{y_i - y_i'}{y_i} \right|}{n} \quad (5)$$

Table 13 shows the output of the error statistics calculation. The average residual was close to 0 (-.244) and the mean absolute percentage error (MAPE) was 6.2 %. Moreover, coefficient of determination from the scatter plot between the observed and the predicted was .882 (Figure 9), representing over 88% of variance in the observed CD IRs was explained by the corresponding bivariate regression model. From this, the SBR models are considered reasonably acceptable. Also, the alternative way of using individual ANs IR within each CD boundary for estimating CD peak cooling energy uses was confirmed methodologically.

Table 13. The error statistics between the predicted and the observed Sqrt of average CD IR for August 2015 in each city district's AWS 1km boundary

Error statistics	Sqrt CD Avg. IR
MAE	.538
MSE	.443
RMSE	.665
MAPE	.062
R^2	.882
Residuals (%)	
Min. residual	-1.294
Max. residual	1.410
Avg. residual	-.244

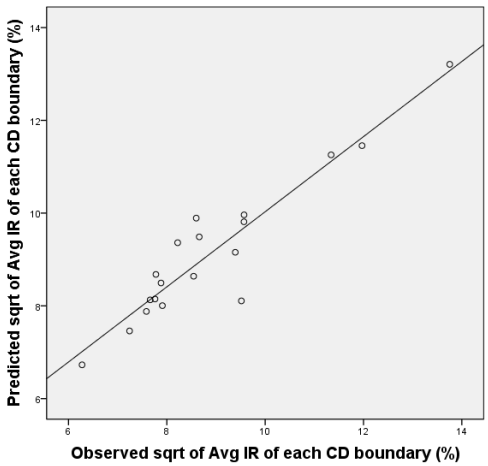

Figure 9. Scatter plot between the predicted and the observed Sqrt of average CD IR for August 2015 in each city district's AWS 1km boundary

To assess the behaviour (bias) of the two residuals—relatively changed or unchanged, a comparative analysis between 2012-14 (training) and 2015 (testing) was conducted on the residuals between predicted and

observed AN IR in each CD. Figure 10 shows the outputs of the comparative analysis: the training residuals for 2012-14 are in black, and the testing for 2015 are in red.

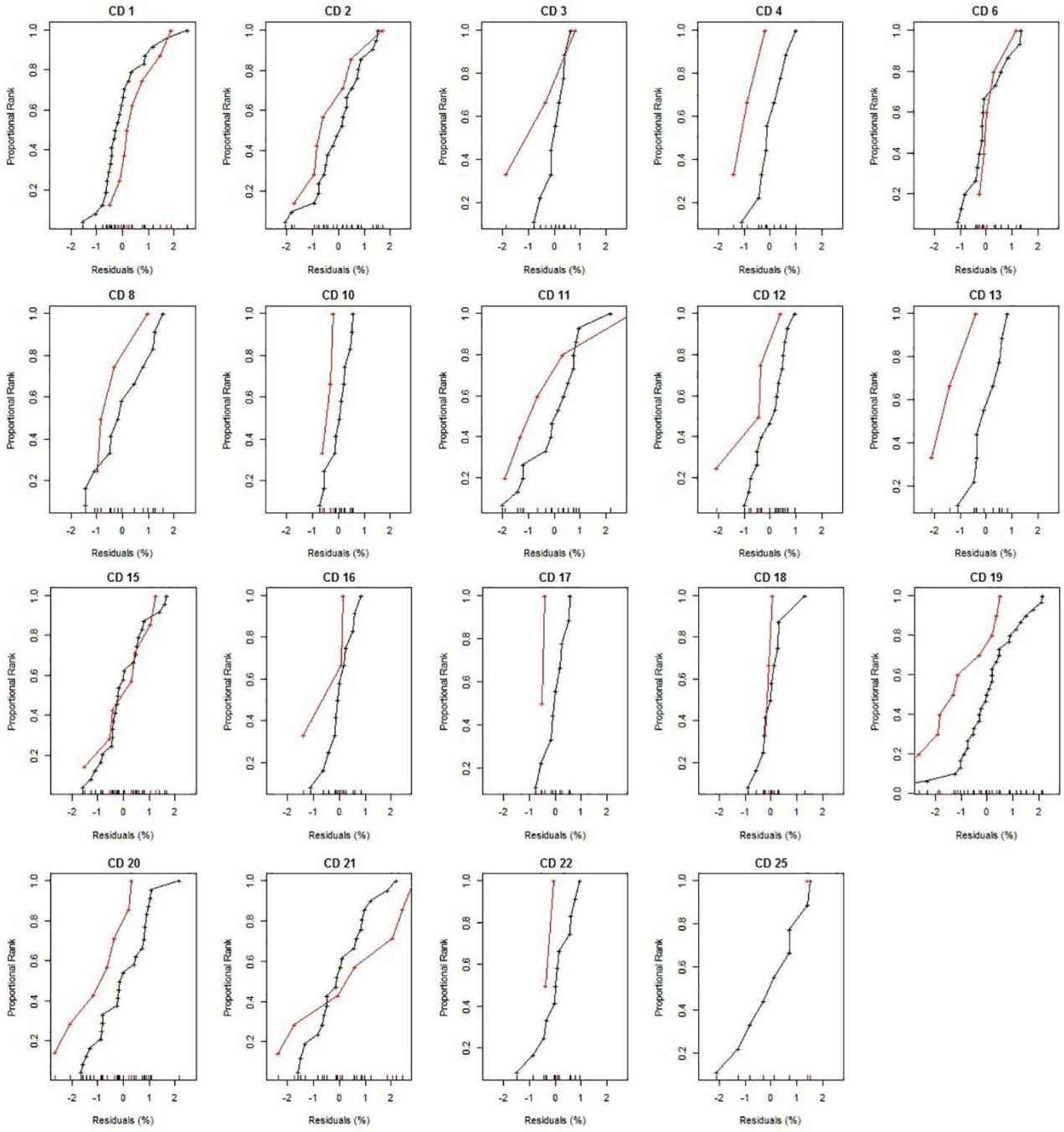

Figure 10. Comparative analysis of residuals between observed and estimated Sqrt average IR of each city district's (CD's) AWS 1km boundary for August 2012-14 (in black as the training set) and 2015 (in red as the testing set)

Firstly, we inspect bias between red and black line. Some CDs, such as CD4, 10, 12, 13, 17, 19, 20, show that all 2015 residuals (red) are to the left of 2012-14 (black), meaning 2015 had lower residuals than 2012-14. This suggests that the predicted energy use (Sqrt IR) for those CDs could be underestimated. CD2, 3, 8 might

be similar to those CDs because only one 2015 residual in each case was right-biased slightly towards 2012-14. Secondly, some CDs had a very similar behaviour between the two residuals, such as CD1, 6, 15, 18, showing similar fit in 2015 to 2012-14 and most of the 2015 residuals were close to 0, meaning the predicted residuals were similar to the observed. This implies that the predicted energy uses in these CDs are reasonably confident. Hence, CD16 and CD22 could be similar to these CDs because their 2015 residuals were near to zero even though left-biased.

Finally, some CDs (CD11, 21, 25) are inconclusive. In CD11, most of 2015 residuals were left-biased but the max residual was largely right-biased. Given the small sample size, it is difficult to draw any conclusion. In CD21, the 2015 residuals were more widely distributed compared to 2012-14, meaning that less variation explained by the model in 2015 than in 2012-14. CD 25 is a special case where very little can be said due to lack of data for 2015.

4.5.3. Projection of future peak cooling demands incorporating climate change projections

Bearing in mind the limitation on accuracy and reliability, the SBR models presented in Table 12 can be applied to estimating future summer peak energy demand if future urban climate projections are available. For the city districts in Seoul, climate change projections generated by MK-PRISM (Modified Korean Parameter-elevation Regressions on Independent Slopes Model) is available and two RCP (Representative Concentration Pathways) scenarios were selected for this study: RCP4.5 and RCP8.5. RCP4.5 is the scenario of CO_2 concentration reaching at 540 ppm in 2100, while RCP8.5 at 940 ppm. We identified the hottest August of the year in both scenarios within 2050s using monthly average temperature between 19th of July and 18th of August. Assuming the same meter-reading day for electricity bill, the temperature projections for 2045 (RCP 8.5) and 2047 (RCP 4.5) were generated.

Figure 11 shows the projected August average temperatures and future peak cooling demands predicted by the SBR models. The 2012 Temp-IR profiles (being the hottest year during 2012-14) are included for reference. As discussed in section 3.5.2, we highlighted the confidence level using different colours: red for underestimated; blue for reasonably confident: black for non-defined confidence.

As the MK-PRISM climate change dataset was produced with a horizontal resolution of 1km x 1km and the CD-AWS data of 2000-2010, the range of temperature changes between 2012 and 2047 (or 2045) varies

across the city districts. For instance, the minimum increase of temperature between 2012 and 2047 occurs in CD25 (0.03°C) while the maximum occurs in CD2 (2.43°C). Secondly, the projection of cooling energy use (IR) is more dynamic and complex. For example, the predicted min and max IR increase occurs in CD17 (6%, underestimated) and CD2 (96.1%, underestimated) respectively, indicating that the predicted cooling energy increase may not always align with projected temperature increase in a linear manner (CD 17 is not projected to have the lowest temperature rise between 2012 and 2045/47, as seen in Figure 11).

Finally, a comparison between the min (CD17) and max (CD21) cooling demands predicted for future years points to a potential challenge/threat to resident's health and well-being living in CD17 if the neighbourhood environment stays largely unchanged. Although the August average temperature of CD17 and CD21 in 2012 (2047) was 27.61°C (29.46°C) and 28.74°C (29.94°C), and the IR was 51.5% (57.5%) and 224.9% (292.8%), the cooling energy bill of CD21 was predicted to increase by 67.9% due to an increase of 1.2°C, while CD17 was predicted to increase by merely 6% in response to an increase of 1.85°C. Here we see a potentially significant negative impact on the health and well-being of residents living in CD17: potential high indoor temperatures lasting for a protracted period of time without adequate cooling energy uses.

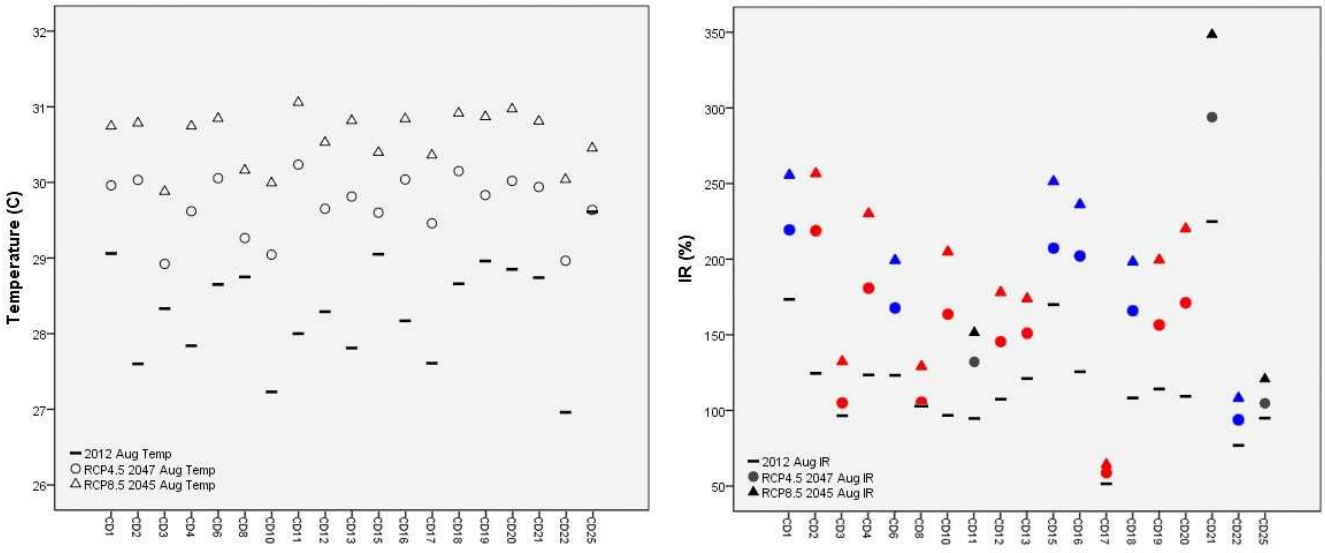

Figure 11. Projected August average temperature (left) and predicted future peak (August) cooling demands (right) in each of city districts' AWS 1km boundary using two different climate change RCP scenarios, RCP4.5 (2047) and RCP8.5 (2045): red for underestimated; blue for reasonably confident; black for non-defined confidence.

5. Conclusion and Further research

5.1. The temporal (monthly) variations

The relationship between cooling energy use and the two factors, urban microclimate data (i.e., monthly average temperature) and property price data, was explored in the analyses of all 98 ANs across the 19 CDs' 1km boundaries at the macro-level. The cooling energy use was very strongly correlated with both of the two factors for the whole summer period (July to September): urban microclimate (r=.770); property price (r=.712). However, there were significant temporal variations in the strength of correlation coefficients in each summer month. Firstly, it was found that there were temporal variations in correlating cooling energy use with urban microclimate data: July (r=.574); August (r=.749); September (r=-.009). Secondly, the correlation coefficients between cooling energy use and property price also had temporal differences: July (r=.698); August (r=.708); September (r=.101). Thirdly, the combined effect of urban microclimate and property price on cooling energy use varied in each summer month: in July, the impact of property price (Beta, .485) was more influential on cooling energy use than urban weather (.331) while the urban weather (.679) was more dominant than property price (.314) in August. This implies that under the high temperature of August, the influence of weather condition on cooling energy use is more dominant than that of the property price (as reflecting socio-economic backgrounds). But under lower temperature of July, the socio-economic factor appears more dominant.

5.2. The temporal and spatial variations

Zooming into the micro-level, there were unique characteristics of cooling energy use within each of the 19 CD boundaries. It was found that the difference in cooling energy use of the 19 CDs was statistically significant (p=.000 in all summer months). Moreover, there were very good internal consistency and similarity in terms of the distribution of monthly cooling energy use within each CD boundary. This implies that there are certain aspects which affect a similar range of cooling energy use in each CD boundary, such as homogeneous microclimatic conditions or socio-economic factors. Given the characteristics, the relational study between cooling energy use and microclimate data was explored within each CD's AWS 1km boundary. There were not only temporal (monthly) variations in relationship between the two variables, but also spatial (each CD) variations. This suggests that the residential cooling energy use should be individually studied within each CD AWS boundary to reflect its own characteristics of cooling energy use.

5.3. Implications of the projected future peak cooling demands

Despite the temporal and spatial variations, it was commonly found that all CDs had the strongest correlation coefficients for August. We generated simple bivariate regression (SBR) model for each CD to estimate future peak cooling energy demands. Given Seoul's MK-PRISM climate change projections made at the CD level, we produce estimates of neighbourhood-specific peak cooling energy demands for future years. The range of temperature changes between 2012 and 2047 (or 2045) varied across the 19 CD boundaries. Moreover, following the temperature diversity and the SBR model in each CD boundary, the projection of cooling energy use was more dynamic and complex, for instance CD17 and CD21: while the increased temperature from 2012 to 2047 (RCP4.5) was 1.85^{o}C (CD17) and 1.2^{o}C (CD21), the increased IR was predicted to only 6% at CD17 but 67.9% at CD21. Furthermore, the absolute amount of IR in 2047 was predicted to 57.5% (CD17) but to 292.8% (CD21). This implies that the internal thermal conditions of the apartment buildings in CD17 may be much poorer than those in CD21, affecting residents' health and well-being if they are unable to increase cooling energy uses due to socio-economic constraints.

5.4. Further research

Firstly, the accuracy of energy model to predict peak cooling energy demands remains uncertain due to the small sample size. As the AMIS only started in 2010, going through the system testing period 2010-2013, the study is limited to the energy bill dataset of 2012-14. Also, as the spatial boundary of AWS 1km radius was set according to the urban microclimate scale, the selected number of apartment neighbourhoods within each CD boundary was also limited. So, the temporal and spatial scope set for data collection in this study resulted in small sample size for the statistical analyses. However, if the energy use data can be collected continuously into further years, the sample size will be large enough to conduct more relational analyses and identify other key parameters affecting residential cooling energy use. Therefore, prediction of peak cooling energy demands could perform better through model improvement with an increased sample size.

Secondly, applying the proposed relational analyses framework, further SBR models can be produced at an individual apartment neighbourhood level if urban microclimate data is available for each apartment neighbourhood. In the microclimatic point of view, the scale of urban microclimate could be much smaller than 1km. Although we assumed that the climatic condition within 1km radius of the CD AWS would be similar, in fact there could be diversity of climates even 1km boundary such as solar radiation. Moreover, the energy model can be generated for even single apartment household. The AMIS energy bill data used for extracting IR (%, as the cooling energy use index) was an average monthly energy bill of each apartment neighbourhood

not a single residential household's monthly energy bill, reflecting collective energy use for summer cooling specific to the neighbourhood location. Therefore, this study did not reflect the diversity of households individually. If the energy use data is made accessible at single apartment household level, the proposed method for projecting energy demand in line with future climate can be applied into individual household.

Finally, with regards to improvement of model accuracy, further research will explore multiple regression modelling and other non-linear statistical methods (Zhao & Magoulès, 2012). The extended study should include measurements of other climatic variables in affecting cooling energy use, such as humidity, wind pattern and solar radiation. However, inclusion of such climatic parameters may be challenging because it should meet certain conditions in terms of data homogeneity: temporal and spatial. The temporal scope of this study is monthly time-based and the spatial is of the neighbourhood scale. Assessing impacts of wind pattern and solar radiation on residential cooling energy use will require site-specific spatial data (i.e. around individual apartment complex building) and a narrower time line (i.e. hourly data), considering characteristics of these two parameters. From a microclimatic point of view, the variations of the two parameters are far more dynamic spatially and temporally than temperature. Within the neighbourhood scale and monthly time-line scope, wind pattern and solar radiation cannot be generalized into monthly value. Furthermore, the effect of those climatic variables should be considered incorporating the individual household's building orientation and glazing ratio data. To obtain the data required at this spatial-temporal resolution, computation intensive CFD-based urban microclimate simulation may be necessary.

References

Allegrini, J., Dorer, V. and Carmeliet, J., 2012. Influence of the urban microclimate in street canyons on the energy demand for space cooling and heating of buildings. *Energy and Buildings*, *55*, pp.823-832.

AMIS, Apartment Management Information System, 2010, http://www.k-apt.go.kr/ (accessed on 09.08.2017)

Arnfield, A.J., 2003. Two decades of urban climate research: a review of turbulence, exchanges of energy and water, and the urban heat island. *International journal of climatology*, *23*(1), pp.1-26.

Asimakopoulos, D.N., Assimakopoulos, V.D., Chrisomallidou, N., Klitsikas, N., Mangold, D., Michel, P., Santamouris, M. and Tsangrassoulis, A., 2001. Energy and climate in the urban built environment. M. Santamouris, University of Athens, Greece. ISBN, 1873936907.

Aydinalp, M., Ugursal, V.I. and Fung, A.S., 2002. Modeling of the appliance, lighting, and space-cooling energy consumptions in the residential sector using neural networks. *Applied Energy*, *71*(2), pp.87-110.

Boo, K.O., Kwon, W.T. and Baek, H.J., 2006. Change of extreme events of temperature and precipitation over Korea using regional projection of future climate change. *Geophysical Research Letter 33*(1).

Bouyer, J., Inard, C. and Musy, M., 2011. Microclimatic coupling as a solution to improve building energy simulation in an urban context. *Energy and Buildings*, *43*(7), pp.1549-1559.

Bronson, D.J., Hinchey, S.B., Haberl, J.S. and O'Neal, D.L., 1992. Procedure for calibrating the DOE-2 simulation program to non-weather-dependent measured loads. In *ASHRAE Winter Meeting, Anaheim, CA, USA, 01/25-29/92* (pp. 636-652).

Catalina, T., Iordache, V. and Caracaleanu, B., 2013. Multiple regression model for fast prediction of the heating energy demand. *Energy and Buildings*, *57*, pp.302-312.

Chan, A.L.S., 2011a. Developing a modified typical meteorological year weather file for Hong Kong taking into account the urban heat island effect. *Building and Environment*, *46*(12), pp.2434-2441.

Chan, A.L.S., 2011b. Developing future hourly weather files for studying the impact of climate change on building energy performance in Hong Kong. *Energy and Buildings*, *43*(10), pp.2860-2868.

Chen, J., Wang, X. and Steemers, K., 2013. A statistical analysis of a residential energy consumption survey study in Hangzhou, China. *Energy and Buildings*, *66*, pp.193-202.

Chung, Y.S., Yoon, M.B. and Kim, H.S., 2004. On climate variations and changes observed in South Korea. *Climatic Change*, *66*(1-2), pp.151-161.

CIP, Climate Information Portal, 2017, http://www.climate.go.kr/index.html (accessed on 09.08.2017)

Collins, L., Natarajan, S. and Levermore, G., 2010. Climate change and future energy consumption in UK housing stock. *Building Services Engineering Research and Technology*.

Crawley, D.B., 2008. Estimating the impacts of climate change and urbanization on building performance. *Journal of Building Performance Simulation*, *1*(2), pp.91-115.

de La Flor, F.S. and Domınguez, S.A., 2004. Modelling microclimate in urban environments and assessing its influence on the performance of surrounding buildings. *Energy and buildings*, *36*(5), pp.403-413.

De Wilde, P. and Coley, D., 2012. The implications of a changing climate for buildings. *Building and Environment*, *55*, pp.1-7.

Frank, T., 2005. Climate change impacts on building heating and cooling energy demand in Switzerland. *Energy and buildings*, *37*(11), pp.1175-1185.

Gaterell, M.R. and McEvoy, M.E., 2005. The impact of climate change uncertainties on the performance of energy efficiency measures applied to dwellings. *Energy and buildings*, *37*(9), pp.982-995.

Grell, G.A., Dudhia, J. and Stauffer, D.R., 1994. A description of the fifth-generation Penn State/NCAR mesoscale model (MM5).

Hacker, J.N., De Saulles, T.P., Minson, A.J. and Holmes, M.J., 2008. Embodied and operational carbon dioxide emissions from housing: a case study on the effects of thermal mass and climate change. *Energy and Buildings*, *40*(3), pp.375-384.

He, J., Hoyano, A. and Asawa, T., 2009. A numerical simulation tool for predicting the impact of outdoor thermal environment on building energy performance. *Applied Energy*, *86*(9), pp.1596-1605.

KAB, Korea Appraisal Board, 2015, Information Service of Publicly Noticed Value of Real Estate Price. http://www.realtyprice.kr/notice/town/searchPastYear.htm (accessed on 09.08.2017)

KAB, Korea Appraisal Board, 2017, http://www.kab.co.kr/kab/home/main/main.jsp (accessed on 09.08.2017)

KEPCO, Korea Electric Power Corporation, 2016, http://home.kepco.co.kr/kepco/main.do (accessed on 09.08.2017)

Kim, D.W., Chung, K.S., Kim, Y.I. and Kim, S.M., 2013b. A comparative study on heating energy consumption for apartment based on the annually strengthened criteria of insulation. *Journal of Energy Engineering*, *22*(2), pp.83-89. [In Korean]

Kim, M.K., Han, M.S., Jang, D.H., Baek, S.G., Lee, W.S., Kim, Y.H. and Kim, S., 2012. Production technique of observation grid data of 1 km resolution. *Journal of climate research*, *7*(1), pp.55-68. [In Korean]

Kim, M.K., Lee, D.H. and Kim, J., 2013a. Production and validation of daily grid data with 1 km resolution in South Korea. *Journal of Climate Research*, *8*(1), pp.13-25. [In Korean]

Kim, S.B., Park, J.H. and Yang, B.E., 2010. A Study on Glazing Ratio of Certified Green Building Apartment. *KIEAE Journal*, *10*. [In Korean]

KMA, Korea Meteorological Administration, 2014, Statistical analysis of climate, http://www.kma.go.kr/weather/climate/stats.jsp (accessed on 09.08.2017)

KMA, Korea Meteorological Administration, 2017, Automatic Weather Station (AWS). http://www.kma.go.kr/weather/observation/aws_table_popup.jsp (accessed on 09.08.2017)

Kolokotroni, M., Giannitsaris, I. and Watkins, R., 2006. The effect of the London urban heat island on building summer cooling demand and night ventilation strategies. *Solar Energy*, *80*(4), pp.383-392.

KOSIS, Korean Statistical Information Service, 2013, http://kosis.kr/statisticsList/statisticsList_01List.jsp?vwcd=MT_ZTITLE&parentId=H#SubCont (accessed on 09.08.2017)

Lee, K., Baek, H.J. and Cho, C., 2014. The estimation of base temperature for heating and cooling degree-days for South Korea. *Journal of Applied Meteorology and Climatology*, *53*(2), pp.300-309.

Lee, K.H. and Levermore, G.J., 2010. Weather data for future climate change for South Korean building design: analysis for trends. *Architectural science review*, *53*(2), pp.157-171.

Lee, S.H. and Baik, J.J., 2010. Statistical and dynamical characteristics of the urban heat island intensity in Seoul. *Theoretical and Applied Climatology*, *100*(1-2), pp.227-237.

Li, D.H., Yang, L. and Lam, J.C., 2012. Impact of climate change on energy use in the built environment in different climate zones–a review. *Energy*, *42*(1), pp.103-112.

MDOP. Meteorological Data Open Portal, 2016, https://data.kma.go.kr/cmmn/main.do (accessed on 09.08.2017)

Moonen, P., Defraeye, T., Dorer, V., Blocken, B. and Carmeliet, J., 2012. Urban Physics: Effect of the micro-climate on comfort, health and energy demand. *Frontiers of Architectural Research*, *1*(3), pp.197-228.

Oke, T.R., 2006. Initial guidance to obtain representative meteorological observations at urban sites, IOM Rep. 81, World Meteorol. *Org., Geneva*.

Rizwan, A.M., Dennis, L.Y. and Chunho, L.I.U., 2008. A review on the generation, determination and mitigation of Urban Heat Island. *Journal of Environmental Sciences*, *20*(1), pp.120-128.

Salvati, A., Roura, H.C. and Cecere, C., 2017. Assessing the urban heat island and its energy impact on residential buildings in Mediterranean climate: Barcelona case study. *Energy and Buildings*, *146*, pp.38-54.

Santamouris, M., Papanikolaou, N., Livada, I., Koronakis, I., Georgakis, C., Argiriou, A. and Assimakopoulos, D.N., 2001. On the impact of urban climate on the energy consumption of buildings. *Solar energy*, *70*(3), pp.201-216.

Santin, O.G., Itard, L. and Visscher, H., 2009. The effect of occupancy and building characteristics on energy use for space and water heating in Dutch residential stock. *Energy and buildings*, *41*(11), pp.1223-1232.

Schuler, A., Weber, C. and Fahl, U., 2000. Energy consumption for space heating of West-German households: empirical evidence, scenario projections and policy implications. *Energy Policy*, *28*(12), pp.877-894.

Seo, K.H. and Lee, L.J., 2011. A white book of Changma. *Korea Meteorological Administration*, *268*.

Tabachnick, Barbara G., and Linda S. Fidell. "Using multivariate statistics, 5th." *Needham Height, MA: Allyn & Bacon* (2007), pp.87.

Touchie, M.F., Binkley, C. and Pressnail, K.D., 2013. Correlating energy consumption with multi-unit residential building characteristics in the city of Toronto. *Energy and Buildings*, *66*, pp.648-656.

Wang, B., Jhun, J.G. and Moon, B.K., 2007. Variability and singularity of Seoul, South Korea, rainy season (1778-2004). *Journal of climate*, *20*(11), pp.2572-2580.

Wang, X., Chen, D. and Ren, Z., 2010. Assessment of climate change impact on residential building heating and cooling energy requirement in Australia. *Building and Environment*, *45*(7), pp.1663-1682.

Yang, X., Zhao, L., Bruse, M. and Meng, Q., 2012. An integrated simulation method for building energy performance assessment in urban environments. *Energy and buildings*, *54*, pp.243-251.

Yu, Z., Fung, B.C., Haghighat, F., Yoshino, H. and Morofsky, E., 2011. A systematic procedure to study the influence of occupant behavior on building energy consumption. *Energy and Buildings*, *43*(6), pp.1409-1417.

Yun, G.Y. and Steemers, K., 2011. Behavioural, physical and socio-economic factors in household cooling energy consumption. *Applied Energy*, *88*(6), pp.2191-2200.

Zhao, H.X. and Magoulès, F., 2012. A review on the prediction of building energy consumption. *Renewable and Sustainable Energy Reviews*, *16*(6), pp.3586-3592.